PERGAMON

Computers and Structures 80 (2002) 1503–1509

Computers & Structures

www.elsevier.com/locate/compstruc

Frequency and time domain dynamic structural analysis: convergence and causality

F. Venancio Filho [a,*], A.M. Claret [b], F.S. Barbosa [c]

[a] Department of Civil Engineering, Pontificial Catholic University of Rio de Janeiro, PUC-Rio, 22453-900 Rio de Janeiro, Brazil
[b] Department of Civil Engineering, School of Mines, Federal University of Ouro Preto, 35400-000 Ouro Preto, MG, Brazil
[c] Department of Civil Engineering, COPPE, Federal University of Rio de Janeiro, 21945-970 Rio de Janeiro, Brazil

Received 2 June 2001; accepted 4 May 2002

Abstract

Matrix formulations for the dynamic analysis of SDOF systems in frequency and time domain are presented in this paper. The strict correspondence between both types of analysis are discussed. A study of the convergence of the response obtained through the frequency domain is performed. This study indicates the presence of an imaginary term in the response when the number of sampling terms in the Fourier transforms is even. A proof of the important causality property of the response is developed and an eventual source of non-causality is indicated.

Keywords: Frequency domain; Time domain; Fourier transforms; Convergence; Causality; Dynamic responses

1. Introduction

The dynamic analysis of structural systems can be performed by time-domain (TD) and by frequency-domain (FD) methods. TD methods stem from the unit-impulse transfer function and the convolution integral while FD methods stem from the complex frequency response function through Fourier transforms (FTs). The strict relation between both methods is a consequence that the unit-impulse transfer function and the complex-frequency response function constitute a pair of FTs.

Venancio-Filho and Claret [1] developed a matrix formulation for the FD analysis of SDOF systems through the concept of implicit Fourier transform (ImFT) or complex-frequency response matrix. According to this concept the direct and inverse discrete FT's are implicitly performed by a compact and elegant matrix expression. Moreover, the number of sampling intervals in the FTs, N, can be arbitrarily selected. Conversely, in the most common fast Fourier transform (FFT) algorithms N must be a power of 2. In this way, with the ImFT formulation the analyst has more flexibility in the selection of the number of sampling intervals. It was also indicated in [1] that, when N is even, a complex term appears in the response. In the present paper a proof of convergence is given which indicates that, with N increasing to infinity, the modulus of that complex term tends to zero and the calculated response tends to the real solution. Numerical results support these conclusions.

Clough and Penzien [2] foresaw the great potentialities of FD methods in dynamic structural analysis. In [3] they provide a thorough treatment of FD methods for SDOF and MDOF systems. Lundén and Dahlberg [4], Karlsson [5], Kumar and Xia [6] and Hall and Beck [7] cover other pertinent aspects of FD methods in dynamic analysis.

The matrix formulation of the TD analysis of SDOF systems is herein presented through the unit-impulse response matrix. The relation between this matrix and the complex-frequency response matrix is established which emphasizes again the strict compatibility between

* Corresponding author. Tel.: +55-21-511-4497; fax: +55-21-511-1546.
E-mail address: fvenanci@civ.puc-rio.br (F.V. Filho).

0045-7949/02/$ - see front matter
PII: S0045-7949(02)00103-7

both methods. Finally, a proof of the important causality property of the response in TD and FD methods is presented.

Recently Mansur et al. [8] presented a very efficient method for the FD linear and non-linear dynamic structural analysis. The ImFT concept is employed in order to solve the dynamic equilibrium equations in modal coordinates, and a time segmentation technique is used for non-linear analysis. On the other hand systems with frequency-dependent properties, like interaction systems (soil–structure, fluid–structure) and with hysteretic damping can be rigorously analyzed only by FD methods. This is an important asset of these methods which is not present in TD methods [8,9].

2. Matrix formulation of frequency-domain analysis

The response of a SDOF system is obtained through a FD analysis by the ImFT concept. This concept is expressed by the following equation [1]:

$$v = \frac{1}{N}\boldsymbol{E}^{*}\boldsymbol{H}\boldsymbol{E}\boldsymbol{p} = \frac{1}{N}\boldsymbol{e}\boldsymbol{p} \tag{1}$$

where $\boldsymbol{e}$ is the complex-frequency response matrix. This matrix has the physical meaning of a SDOF dynamic flexibility matrix as it transforms the load time history into the corresponding response time history.

In Eq. (1)

$$\boldsymbol{p} = \{p(t_0), p(t_1), p(t_2), \ldots, p(t_n), \ldots, p(t_{N-1})\}^t \tag{2}$$

is the vector of the excitation at the discrete time instants $t_n = n\Delta t = nT_\mathrm{p}/N (n = 0, 1, 2, \ldots, N-1)$, and

$$v = \{v(t_0), v(t_1), v(t_2), \ldots, v(t_n), \ldots, v(t_{N-1})\}^t \tag{3}$$

is the vector of the response at the corresponding discrete times; $\boldsymbol{E}$ and $\boldsymbol{E}^*$ are $(N \times N)$ matrices whose generic terms are, respectively, $E_{mn} = \mathrm{e}^{-\mathrm{i}mn(2\pi/N)}$ and $E^*_{mn} = \mathrm{e}^{\mathrm{i}mn(2\pi/N)}$; $\boldsymbol{H}$ is a $(N \times N)$ diagonal matrix composed with the complex frequency response functions at the discrete frequencies $\Omega_m = m\Delta\Omega = m(2\pi/T_\mathrm{p})$ $(m = 0, 1, 2, \ldots, N-1)$; and T_p is the extended period. The generic term of $\boldsymbol{H}$ is

$$H(\Omega_m) = \left\{k\left[\left(1-\beta_m^2\right) + \mathrm{i}(2\xi\beta_m + \operatorname{sgn}\beta_m\lambda)\right]\right\}^{-1} \tag{4}$$

where k is the system stiffness; $\beta_m = \Omega_m/\omega = m(\Delta\Omega/\omega)$; ω is the natural frequency, ξ is the damping ratio; and λ is the hysteretic damping factor. The discrete frequencies Ω_m must be considered in accordance with Tables 1 and 2 where the symmetry of positive and negative frequencies is expressed. It is worthwhile to mention that the complex frequency response function of Eq. (4) can take into account viscous and hysteretic damping.

Table 1
Discrete frequencies (N odd)

m	Ω_m
0	0
1	$\Delta\Omega$
2	$2\Delta\Omega$
...	...
$(N-1)/2$	$[(N-1)/2]\ \Delta\Omega$
$(N+1)/2$	$[-(N-1)/2]\ \Delta\Omega$
...	...
$N-2$	$-2\Delta\Omega$
$N-1$	$-\Delta\Omega$

Table 2
Discrete frequencies (N even)

m	Ω_m
0	0
1	$\Delta\Omega$
2	$2\Delta\Omega$
...	...
$(N/2)-1$	$[(N/2)-1]\ \Delta\Omega$
$(N/2)$	$(N/2)\Delta\Omega$
$(N/2)+1$	$-[(N/2)-1]\ \Delta\Omega$
...	...
$N-2$	$-2\Delta\Omega$
$N-1$	$-\Delta\Omega$

3. Matrix formulation of time-domain dynamic analysis

The TD analysis is performed through the unit-impulse transfer function $h(t)$ which is the inverse FT of the complex-frequency transfer function $H(\Omega)$. Then, by definition,

$$h(t) = \frac{1}{2\pi}\int_{-\infty}^{+\infty} H(\Omega)\mathrm{e}^{\mathrm{i}\Omega t}\,\mathrm{d}\Omega. \tag{5}$$

$h(t)$ is the unit-impulse response function. Its physical interpretation is that it provides the response of a SDOF due to a unit impulse.

The discrete form of Eq. (5) is

$$h(t_s - t_r) = h_{sr} = \frac{\Delta\Omega}{2\pi}\sum_{m=0}^{N-1} H(\Omega_m)\mathrm{e}^{\mathrm{i}\Omega_m(t_s-t_r)}. \tag{6}$$

Taking into account that $t_s = s\Delta t$, $t_r = N\Delta t$, and $\Omega = m\Delta\Omega$ and separating the positive and negative exponents, Eq. (6) transforms into

$$h(t_s - t_r) = h_{sr} = \frac{\Delta\Omega}{2\pi}\sum_{m=0}^{N-1} \mathrm{e}^{\mathrm{i}sm\frac{2\pi}{N}} H(\Omega_m)\mathrm{e}^{-\mathrm{i}rm\frac{2\pi}{N}}. \tag{7}$$

Introducing now the $(N \times N)$ matrices $\boldsymbol{E}^*$ and $\boldsymbol{E}$ whose generic terms are $E^*_{sm} = \mathrm{e}^{\mathrm{i}sm(2\pi/N)}$ and $E_{mr} = \mathrm{e}^{-\mathrm{i}rm(2\pi/N)}$, respectively, and the $(N \times N)$ diagonal matrix $\boldsymbol{H}$ defined through Eq. (4) leads to the following expression for the unit-impulse transfer matrix:

$$\boldsymbol{h} = \frac{\Delta\Omega}{2\pi}\boldsymbol{E}^{*}\boldsymbol{H}\boldsymbol{E}. \tag{8}$$

The substitution of $\boldsymbol{E}^{*}\boldsymbol{H}\boldsymbol{E}$ from the foregoing equation into Eq. (1) and consideration of $\Delta\Omega\,\Delta t/2\pi = 1/N$, gives

$$\boldsymbol{v} = \Delta t\boldsymbol{h}\boldsymbol{p}. \tag{9}$$

Eq. (9) expresses the system response obtained through a TD analysis. The response in the generic time t_s is, from Eq. (9),

$$v(t_s) = \Delta t\sum_{s=0}^{N-1} p(t_r)h(t_s - t_r). \tag{10}$$

Eq. (10) is the discrete form of the convolution equation $v(t) = \int_0^t p(\tau)h(t-\tau)\,\mathrm{d}\tau$.

Comparing now Eqs. (1) and (9) and taking into account that $\Delta\Omega\,\Delta t/2\pi = 1/N$ one obtains

$$\boldsymbol{h} = \frac{1}{\boldsymbol{N\Delta t}}\boldsymbol{e} = \frac{2\pi}{\Delta\Omega}\boldsymbol{e}. \tag{11}$$

Eq. (11) expresses the relation between the ImFT matrix **e** (analysis in the FD domain) and the unit-impulse transfer matrix **h** (analysis in the TD domain).

4. Convergence analysis

The convergence analysis is presented along two lines. Initially, it is shown that, when N is even, there is an complex term in the generic response $v(t_n)$, and then it is proven that this term tends to zero, when N tends to infinity. In the sequel a proof is given that, with increasing N, $v(t_n)$ converges to the real solution.

The generic response $v(t_n)$, in the generic time t_n, is derived from Eq. (1) as

$$v(t_n) = \frac{1}{N}\sum_{m=0}^{N-1} \mathrm{e}^{\mathrm{i}2\pi(mn/N)}H(\Omega_m)\sum_{n=0}^{N-1} p(t_n)\mathrm{e}^{-\mathrm{i}2\pi(mn/N)}. \tag{12}$$

Taking into account the discrete frequencies of Table 1 (N odd), the first summation $(\sum_{m=0}^{N-1})$ in Eq. (12) is a summation of a real term ($m = 0$) with pairs of complex conjugates ($m = 1, \ldots, N-1$) whose generic pair is

$$C_{m,\bar{m}} = \mathrm{e}^{\pm\mathrm{i}2\pi(mn/N)}H(\Omega_m)\sum_{n=0}^{N-1} p(t_n)\mathrm{e}^{\mp\mathrm{i}2\pi(mn/N)} \tag{13}$$

where the subscripts m and $\bar{m}$ correspond, respectively, to positive and negative frequencies (Table 1). When $N$is even (Table 2), the term of highest order in Eq. (12) is a complex term, $C_{N/2}$, associated with the Nyquist frequency, $\Omega_{N/2}$. Substituting $N/2$ for m in Eq. (13) leads to the following expression

$$C_{N/2} = \cos n\pi H(\Omega_{N/2})\sum_{n=0}^{N-1} p(t_n)\cos n\pi. \tag{14}$$

As N is even the summation in the RHS of Eq. (14) can be developed as a summation of pairs as follows:

$$\begin{aligned}\sum_{n=0}^{N-1} p(t_n)\cos n\pi &= [p(t_0) - p(t_1)] + [p(t_2) - p(t_3)] \\ &\quad + \cdots + [p(t_r) - p(t_{r+1})] \\ &\quad + \cdots + [p(t_{N-2}) - p(t_{N-1})],\end{aligned} \tag{15}$$

with r even. All the pairs in the previous equation can be expressed, like the generic one, as

$$[p(t_r) - p(t_{r+1})] = \left[p(t_r) - p\left(t_r + \frac{T_\mathrm{p}}{N}\right)\right]. \tag{16}$$

In the limit, when N tends to infinity, the following result is obtained:

$$\lim_{N\to\infty}\left[p(t_r) - p\left(t_r + \frac{T_\mathrm{p}}{N}\right)\right] = p(t_r) - p(t_r) = 0. \tag{17}$$

Therefore, when N tends to infinity, the central complex term given by Eq. (14) tends to zero. On the other hand it is verified that, due to the first $\cos n\pi$ in Eq. (14), the imaginary part of the response oscillates with changing n. Hall and Beck [7] implicitly suggest the existence of this imaginary term when they write, after Eq. (8) of their paper, *where only the real part of H* $(m\Delta\omega)$ *is used at* $m = N/2$, without any further consideration.

In order to prove that $v(t_n)$, Eq. (12), converges to the exact solution when N tends to infinity, it is only necessary to prove that the pair of complex conjugates of highest order ($n = N - 1 = R$) tends to zero when N tends to infinity. This pair is, from Eq. (12),

$$C_{R,-R} = \mathrm{e}^{\pm\mathrm{i}2\pi\frac{N-1}{2}\frac{n}{N}}H(\Omega_{R,-R})\sum_{n=0}^{N-1} p(t_n)\mathrm{e}^{\mp\mathrm{i}2\pi\frac{N-1}{2}\frac{n}{N}}. \tag{18}$$

When N tends to infinity the exponents in Eq. (18) tend to $\mathrm{i}2\pi n$. In this way this equation is transformed into

$$C_{R,-R} = \cos\ n\pi H(\Omega_{R,-R})\sum_{n=0}^{N-1} p(t_n) cos\ n\pi. \tag{19}$$

The modulus of the sum of the complex conjugates in Eq. (19) is

$$\begin{aligned}P &= C_R + C_{-R} \\ &= 2\cos n\pi\left[\frac{1}{k\left[\left(1-\beta_R^2\right) + (2\varsigma\beta_R + \lambda)^2\right]^{1/2}}\right] \\ &\quad\times\sum_{n=0}^{N-1} p(t_n)\cos n\pi.\end{aligned} \tag{20}$$

Considering now that the summation in this equation tends to zero when N tends to infinity according to Eqs. (15)–(17) and that, in face of damping, the term in brackets is limited, even when $\beta_R = 1$, i.e., Ω_R coincides eventually with the natural frequency, P tends to zero when N tends to infinity. Thus, it is finally proven that $v(t_n)$, Eq. (12), tends to the exact solution when N tends to infinity.

5. Causality of the response

The causality of the response is the property that the response at any time $t$is not influenced by the excitation at all the times greater than t. With the consideration of Eqs. (1) and (9) the causality property corresponds to the lower triangularity of matrices $\boldsymbol{e}$ and $\boldsymbol{h}$. In order that $\boldsymbol{h}$ be lower triangular the load $p(t_r)$ $(r > s)$ should not contribute to the response at time t_s which is equivalent to $h(t_s - t_r) = 0$ for $r > s$. To prove this, consider Eq. (7) with the exponents gathered

$$h(t_s - t_r) = h_{sr} = \frac{\Delta\Omega}{2\pi} \sum_{m=0}^{N-1} H(\Omega_m) \mathrm{e}^{-\mathrm{i}m(r-s)\frac{2\pi}{N}}. \tag{21}$$

The maximum absolute value of $H(\Omega_m)$ occurs when, eventually, $\Omega_m = \omega$. Then, from equation

$$|H(\Omega_m)|_{\max} = |H(\omega)| = \frac{1}{k(2\xi + \lambda)}. \tag{22}$$

Therefore the following inequality is verified:

$$|H(\Omega_m)| \leqslant |H(\omega)|. \tag{23}$$

Introducing this inequality into Eq. (21), the modulus $|h_{sr}|$ of h_{sr} is expressed as

$$|h_{sr}| \leqslant \frac{\Delta\Omega}{2\pi} |H(\omega)| \left| \sum_{m=0}^{N-1} Z_m \right| \tag{24}$$

where

$$Z_m = \mathrm{e}^{-\mathrm{i}m(r-s)\frac{2\pi}{N}} (r > s). \tag{25}$$

Now, $\sum Z_m$ from Eq. (24) is a geometric series with ratio $Z = \mathrm{e}^{-\mathrm{i}(r-s)\frac{2\pi}{N}}$ and it is proven in Ref. [10] that it is absolutely convergent, i.e.,

$$1 + Z + Z^2 + \cdots + Z^N = \frac{1 - Z^{\mathrm{N}}}{1 - Z} (Z \neq 1). \tag{26}$$

On the other hand, from Eq. (25), $Z^N = 1$. Then, from Eq. (26) the series $\sum Z_m$ converges to zero. In consequence, from Eq. (25), the terms such as $h_{sr}(r > s)$ converge to zero as N tends to infinity. This conclusion proves finally the causality of the response of the TD and FD dynamic analysis expressed, respectively, by Eqs. (9) and (1).

In real engineering problems the actual response must be causal and non-causalities are difficult to interpret from an engineering point of view [4]. Crandall [11] demonstrates that, for a particular case of excitation and hysteretic damping, the response is non-causal. On the other hand, one of the main causes of non-causal responses is the insufficient extension of the period. Refs. [6] and [8] propose a fair criterion to obtain an adequate extension of the period. The extended period T_{p} should be taken as

$$T_{\mathrm{p}} = \alpha \frac{\ln 10}{\xi} \tag{27}$$

where ω is the natural frequency ξ the damping ratio and $2 \leqslant \alpha \leqslant 4$.

6. Example

The aims of the first example are (1) to verify the fairly good convergence characteristic of the FD solution as the number of terms in the FT's tends to infinity; (2) to confirm numerically the presence of a complex term in the solution when N is even and the oscilation of its imaginary part with changing n; (3) to indicate the very fast convergence to zero of that imaginary term when N tends to infinity; (4) to show that, with the ImFT formulation, one can take an arbitrary number of terms in the FT's; (5) show that, when the extended period is insufficient, there is some non-causality on the response.

An 1 DOF system with the following properties is considered: stiffness $k = 16,000$ kN/m; mass $m = 100$ kg ; damping ratio $\xi = 0.05$. The system is subjected to a versed-sine pulse with duration of 0.8 T where T is the system natural period. The peak value of the load variation is 100 kN.

Figs. 1–3 depict the perfectly matched responses obtained by ImFT and FFT with $N = 32$, 256 and 1024,

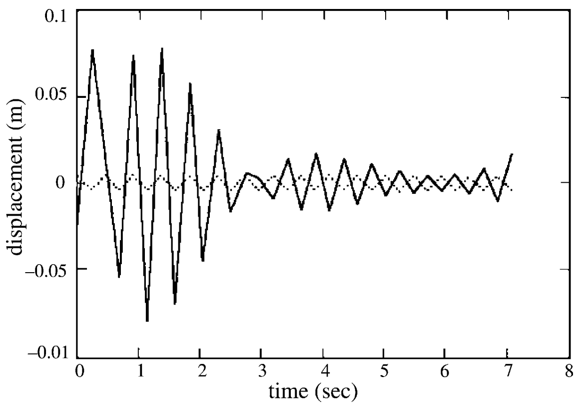

Fig. 1. Response with $N = 32$. (—) real part, (- - -) imaginary part.

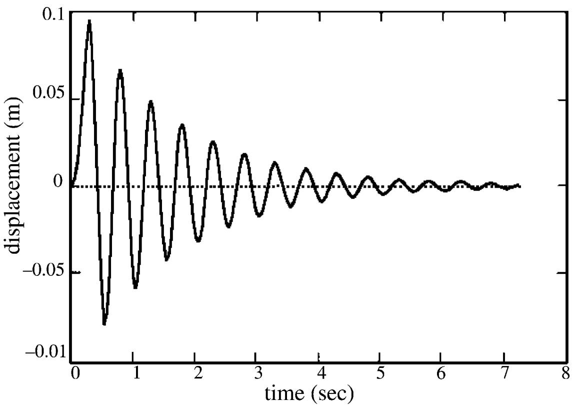

Fig. 2. Response with $N = 256$. (—) real part, (- - -) imaginary part.

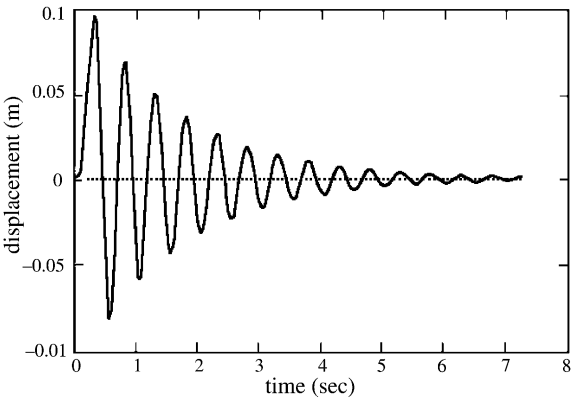

Fig. 3. Response with $N = 1024$. (—) real part, (- - -) imaginary part.

respectively. Moreover the solutions with $N = 256$ and above are the same which indicates the very good convergence characteristics of the FD method. It is important to observe in Fig. 1 the oscillation of the solution imaginary part. Table 3 presents the maximum values of the response with N from 2^5 to 2^{11}. The convergence to the exact solution and the convergence to zero of the imaginary part is fairly good. Figs. 4 and 5 display the

Table 3
Maximum values of the response with $N = 32$–2048

N	Real part (cm)	Imaginary part (cm)
32	0.805	± 0.042
64	0.922	$\pm 2.27 \times 10^{-5}$
128	0.920	$\pm 9.89 \times 10^{-9}$
256	0.956	$\pm 2.66 \times 10^{-10}$
526	0.956	$\pm 7.81 \times 10^{-12}$
1024	0.956	$\pm 2.28 \times 10^{-13}$
2048	0.956	$\pm 6.12 \times 10^{-15}$

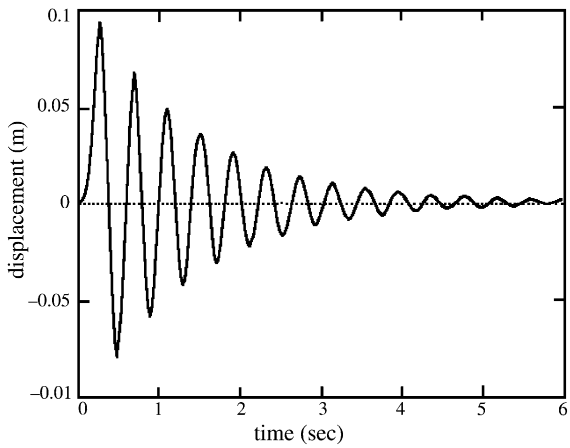

Fig. 4. Response with $N = 325$. (—) real part, (- - -) imaginary part.

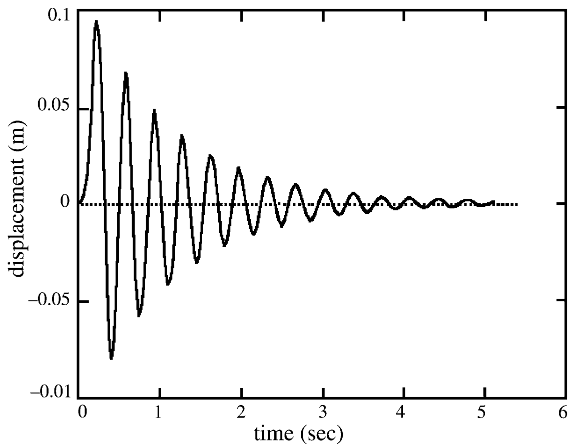

Fig. 5. Response with $N = 600$. (—) real part, (- - -) imaginary part.

responses for arbitrary $N = 325$ and 600, respectively, and Table 4 presents the maximum values of the response for other arbitrary N. The convergence is again

Table 4
Maximum values of the response with arbitrary N

N	Real part (cm)	Imaginary part (cm)
111	0.95	0
256	0.956	2.66×10^{-10}
300	0.957	8.66×10^{-10}
325	0.956	0
600	0.957	1.07×10^{-11}
661	0.956	0
1050	0.957	0
1201	0.956	0

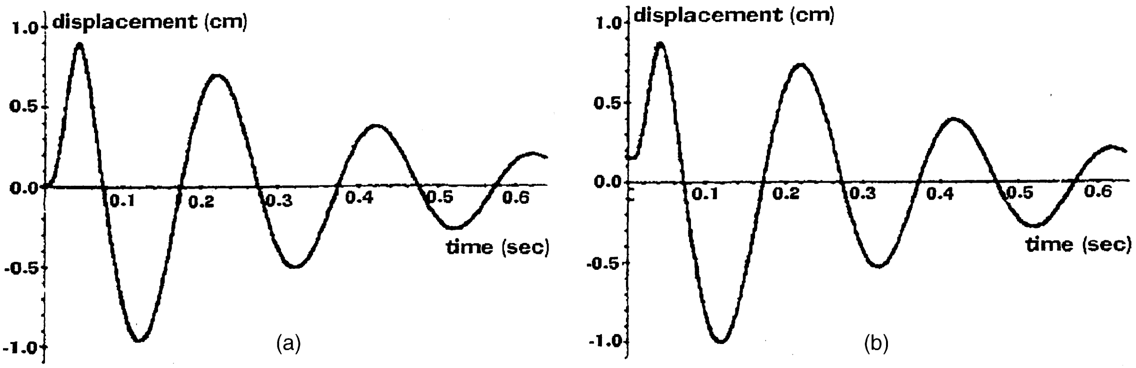

Fig. 6. (a) Causal response and (b) non-causal response.

fairly good and the imaginary part, when N is odd, is always zero.

The second example indicates that, when the extended period is inadequate, the response is non-causal. The response of a SDOF system with natural period $T = 0.20$ s, damping ratio $\xi = 0.03$ submitted to a short-duration half-sine pulse with duration $t_d = 0.03$ s is displayed in Fig. 6a and b. The response in Fig. 6a, obtained with an extended period $T_p = 1.46$ s, calculated according to Eq. (27), is causal. Conversely, the response calculated with an insuficient period $T_p = 0.64$ s is non-causal, Fig. 6b.

7. Conclusion

Matrix formulation for FD and TD dynamic analysis SDOF structural systems were presented. The strict correspondence between the two types of analysis was discussed. The convergence analysis of the response obtained by the FD method indicated that, when N is even, there is a complex term in the response whose imaginary part oscillates and that, with increasing N, the response finds to the exact one. The causality of the response was proven and a possible source of non-causality related to the insufficient extension of the period was pointed out. The given examples support the conclusions of the convergence and causality analyses.

FD domain methods are superposition methods like mode superposition ones. These methods have the advantage over TD methods as they prevent the analysis of vibration frequencies and mode shapes. On the other hand the frequency truncation in FD methods corresponds to the mode truncation in TD methods. From the computational point of view one can not be dogmatic whether one or other method is superior. The computational efficiency depends very much upon the problem and the preference of the analyst. Numerical solutions in the FD through the ImFT concept are competitive with TD ones with regard to accuracy and computational efficiency, as indicated by the examples in [8,9]. In conclusion, FD methods are theoretically consistent and mandatory for rigorous analysis of systems with hysteretic damping and frequency-dependent properties [8,9].

Acknowledgements

The first author acknowledges State of Rio de Janeiro Foundation for Research Support FAPERJ which provided support for this work through grant no. E-26/150.994/2000.

References

[1] Venancio-Filho F, Claret AM. Matrix formulation of the dynamic analysis of SDOF systems in the frequency domain. Comput Struct 1992;42(5):853–5.
[2] Clough RW, Penzien J. Dynamics of structures. New York: McGraw-Hill; 1975.
[3] Clough RW, Penzien J. Dynamics of structures. second ed. New York: McGraw-Hill; 1993.
[4] Lúnden R, Dahlberg T. Frequency-dependent damping in structural vibration analysis by the use of complex series expansion of transfer functions and numerical fourier transformation. J Sound Vib 1982;80(2):161–78.
[5] Karlsson L. Numerical analysis of damped transient beam vibrations by use of Fourier transforms. Int J Numer Meth Eng 1985;21:683–9.
[6] Kumar JL, Xia H. Dynamic response analysis in the frequency domain. Earthquake Eng Struct Dynam 1993; 22:1–12.
[7] Hall JF, Beck JL. Linear system response by DFT: analysis of a recent modified method. Earthquake Eng Struct Dynam 1993;22:599–615.
[8] Mansur WJ, Ferreira WG, Claret AM, Venancio-Filho F, Carrer JAM. Time segmented frequency-domain analysis for non-linear multi-degree-of-freedom structural systems. J Sound Vib 2000;237(3):457–75.

[9] Ferreira WG, Claret AM, Venancio-Filho F, Mansur WG. A frequency-domain pseudo-force method for dynamic structural analysis. Nonlinear systems and nonproportional damping. J Brazilian Soc Mech Sci 2000;XXII(4):551–64.
[10] Solkonikoff IS, Redheffer RM. Mathematics of physics in modern engineering. New York: McGraw-Hill; 1996.
[11] Crandall SH. The role of damping in vibration theory. J Sound Vib 1970;11(1):3–18.